Control of Combustion Instabilities on a Rijke Tube by a Neural Network

R. Blonbou*¶, A. Laverdant *
* Office National d'Études et de Recherches Aérospatiales,
29, avenue de la Division Leclerc,
BP n° 72, 92322 Châtillon Cedex, France.
mail : laverdan@onera.fr
¶ present address : Engineering Department, Cambridge University, Trumpington Street
CB2 1PZ CAMBRIDGE, CAMBRIDGESHIRE, UK.
mail : rhb26@eng.cam.ac.uk

Abstract

Combustion instabilities still constitute a major problem for powerplant development. In this paper, a Rijke tube which presents, for some operating conditions, instabilities with pressure level up to 145 dB/Hz, is considered. In order to control instabilities, an Internal Model Control System for nonlinear plants, that uses two neural networks, has been developed. The first one is an Internal Model which approximates the plant forward dynamic (the learning process). The second one gives the adaptive control input. The capacity of approximating the noisy signals of instabilities (microphone or photomultiplier for OH emission proportional to heat release), with a good precision, is demonstrated. Attenuation of instabilities, for fixed or variable operating conditions, with pressure level attenuation up to 60 dB/Hz, has been obtained.

Introduction

Combustion instabilities represent an important difficulty encountered during the conception of aeronautical or aerospace powerplant [1-4]. These oscillatory mechanisms have disastrous consequences like structure vibrations, increased heat transfer versus stable regime, undesired roll torque and, sometimes, destruction of the powerplant. According to Williams [2], several types of oscillations are observed (system -, intrinsic - or chamber instability). In this paper, only the last case is considered. As an example, in a ramjet, one or several acoustic modes of an air intake and / or chamber, are coupled with unsteady combustion heat release. Here, the burner involved is a Rijke tube with propane-air mixture burning above a porous plate. Similar setups have been considered in previous studies at Cambridge University [5,6] or Ecole Centrale de Paris [7].

The control of instabilities (passive or active) is a natural way to overcome these unwanted oscillations. The first way - the passive control [4,8] - consists in modifying the chamber geometry by the introduction of baffles or Helmholtz resonators which change eigenfrequencies and introduce additional damping of instabilities. Unfortunately, this approach increases mass and dimensions of the powerplant. Moreover, its damping efficiency is limited. The second way - the active control - (see [9] for a good review), consists in the introduction of a secondary acoustic signal with a correct phase shift to obtain a stable regime. The original aspect of the present work is the use of a nonlinear filtering technique : the neural network.

The active control has been used with success to suppress instabilities in laboratory combustors [5-7, 9]. The control loop consists of one or more sensors (microphone or photomultiplier which detects light emission proportional to heat release) [5], a phase shift device and an actuator (generally an electro-pneumatic driver) [9, 10]. The control schemes control unstable modes at sufficiently distant frequencies. Despite of some success, this techniques presents limitations. First, the parameters of the controller are set manually. Secondly, when several modes are present with the same level, the control fails.

In order to overcome this limitation, Huynh *et al.* [10], Billoud *et al.* [11], have used an adaptive control algorithm based upon energy minimization of the global response sensor signal, through optimization of the controller parameters (Widrow [12]). The filter is linear (Infinite Impulse Response -IIR). Different unstable modes are controlled in a 250 kW turbulent burner.

Neumeier and Zinn [13] uses an observer which identifies the unstable modes and determines their phases and amplitudes. These informations are inputs for a controller which stabilizes each unstable mode. This approach has obtained some success for the reconstruction of an unstable pressure signal with transition from low to high frequency. However, the control scheme is limited by the linear modeling of flame response to acoustic perturbations.

More recently, Yu , Wilson and Schadow [14] have used liquid injection (ethanol, heptane and JP 10) to damp combustion instabilities of a dump combustor. Droplets entrainment and flame/large scale vortex interaction limit the damping to 15 dB/Hz. It seems that the injection pass band is limited to several hundred of Hertz. However, this research has given a better understanding of physico - chemical processes involved in an unstable dump combustor.

Paper presented at the RTO AVT Symposium on "Active Control Technology for Enhanced Performance Operational Capabilities of Military Aircraft, Land Vehicles and Sea Vehicles", held in Braunschweig, Germany, 8-11 May 2000, and published in RTO MP-051.

In order to improve the different techniques, we use an artificial neural *network with a non linear algorithm*. This device is a powerful tool and a universal parsimonious approximer for any nonlinear function (Bishop [15]). Neural networks are able to model and control nonlinear plant (Hunt *et al.* [16]). In the present work, an adaptive control strategy, based on Internal Model Control Systems (I.M.C.S.), is presented.

The experiments are made on a Rijke tube [17-20].

The experimental setup is described in paragraph 2. Results without control are presented in paragraph 3. Then, a short description of Artificial Neural Networks (A.N.N.) is proposed in paragraph 4. Results with control are described in paragraph 5 before conclusion in paragraph 6.

2 - Experimental setup [19,20]

Description

Air and propane are injected into the premixed chamber below the flame holder. The ignition is obtained with a high energy spark plug disposed above the porous plate. Four glass windows are set up at right angle at the bottom of the chamber for flame visualization and radical emission measurements.

The experimental setup is shown in Fig. 1. The burner consists in two square section tubes of 50 mm x 50 mm separated by a porous wall made of Poral ®. This porous plate, which acts as a flame holder, is located at 25 cm of the bottom of the tube. Chambers of 75 cm and 1 m lengths have been tested. The tube is closed at the bottom and open at the opposite. This geometry allows only longitudinal acoustic waves to propagate at frequencies below 5 kHz.

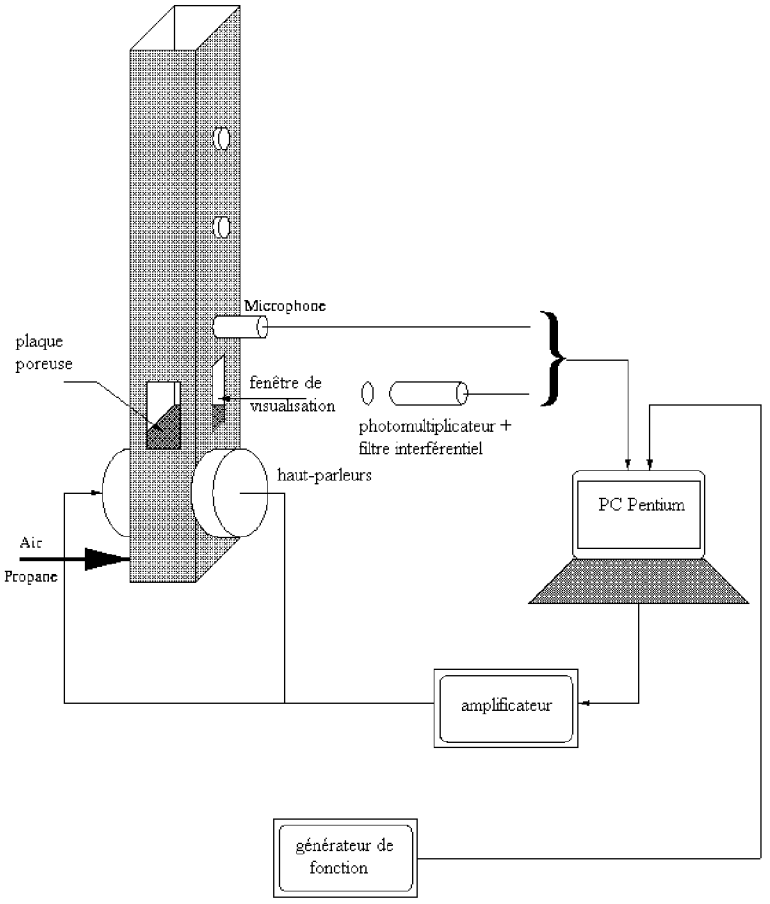

Fig. 1 - Experimental configuration

Measurements

A Chromel-Alumel thermocouple is fitted in the porous plate. Experiments, where temporal temperature variation in the flame holder were above 300 °C/min, have been limited in time in order to avoid porous wall destruction.

Brüel and Kjaer microphones of type 4136 (1/8 ") have been installed along the Rijke tube (maximum pass band starts of 10 kHz).

Diederichsen and Gould [22] have verified that for premixed flames, the intensity of CH, OH or C_2 radical emissions are proportional to the flame heat release. Following Dines [5], OH emission is measured with a photomultiplier tube after rejection of spurious light with an interference filter centered at 310 nm.

Pressure and OH chemiluminescence signals are recorded on a PC computer with a KETLEY data acquisition card.

The actuation system is composed of two electro-pneumatic drivers JBL 2490H (pass band from 100 Hz to 1 kHZ). These drivers are disposed on two opposite walls, below or above the porous plate. The acoustic signals are issued of a Hewlett-Packard function generator. Theses signal are amplified by a JBL MPX 300 amplifier.

3 - Experimental results without control [19]

Configuration and regime tested

Experiments are conducted with flow velocities below 20 cm/s; thus the flame is a laminar one. The equivalence ratio Φ lies between 0.6 and 1.4 and the flame is plane in the majority of cases. In this situation, laminar flame speed is close to 40 cm/s for stoechiometric conditions. So the flame zone is closed to the porous plate. For equivalence ratios between 0.8 and 1.3, large sustained acoustic oscillations are observed. The maximum air mass flow rate is of 0.4 g/s.

The operating conditions are summarized in Table 1. In the following developments, each operating case is referenced as "regime I", *etc.*

regimes	L (mm)	$\dot{m}\acute{Y}_{air}$ (mg/s)	$\dot{m}\acute{Y}_{C3H8}$ (mg/s)	Φ
I	750	250	15.5	1
II	750	300	20	1
III	750	225	15.5	1.1
IV	750	300	15.5	0.8
V	1000	200	13	1
VI	1000	300	25	1.3

Table 1 - Characteristics of operating conditions used in test of active control.

Description of instabilities

Temporal variations of pressure and OH emission signals, in presence of instabilities, are plotted in Figures 2 and 3. The instability presents a limit cycle (Fig. 2). The relative phase between the two signals is close to zero (Fig. 3), in agreement with the Rayleigh's criterion [23].

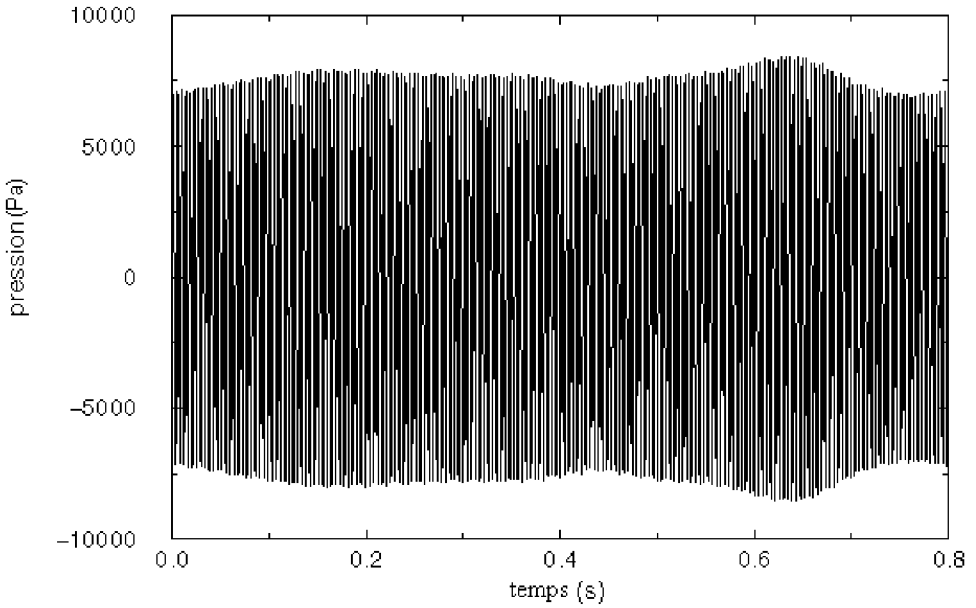

Fig. 2 - Temporal variation of pressure signal in an unstable regime [19].

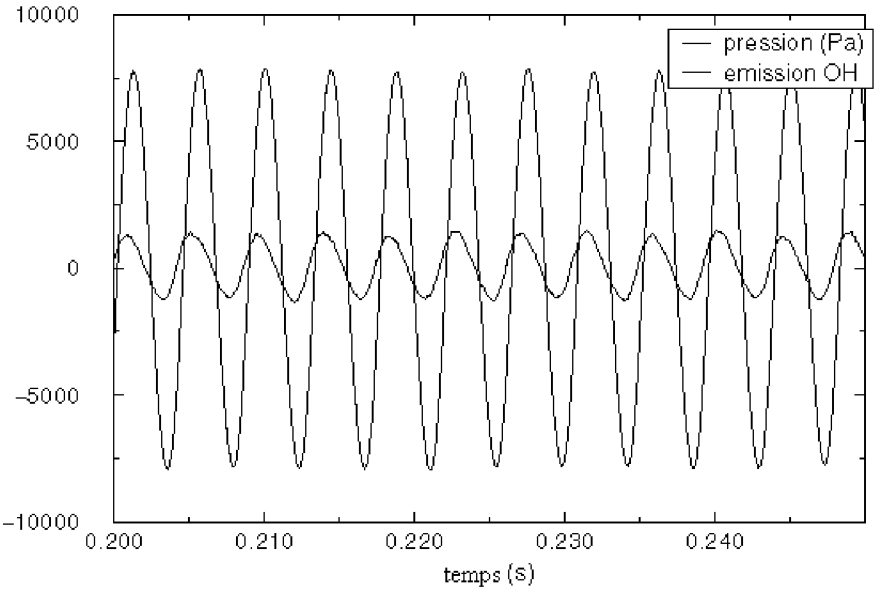

Fig. 3 - Temporal variations of pressure and OH emission for an unstable regime
(pressure is in Pa and OH signal in arbitrary units) [19].

The diagrams of the instability zones, for tube lengths of 75 cm and 1m, are shown in Fig. 4 and 5 respectively. The characteristic of the instabilities depends of several factors :

• the operating point : frequency and amplitude of oscillations vary as a function of this parameter. For a 1m tube length and rich conditions, the oscillations are intermittent.

• porous wall temperature : some instabilities are observed only when $T_{wall} > 100$ °C. When this parameter is greater than 300 ° C, the instabilities observed for high values of Φ are attenuated. This parameter gives only indications on combustion. It is

possible to suppose that increase of porous wall temperature implies growing of fresh mixture temperature also. This variation is quasi-steady and the critical value of 300 °C is reached after a long time of operation.

• operating duration : frequency and amplitude of oscillations can present weak variations with time.

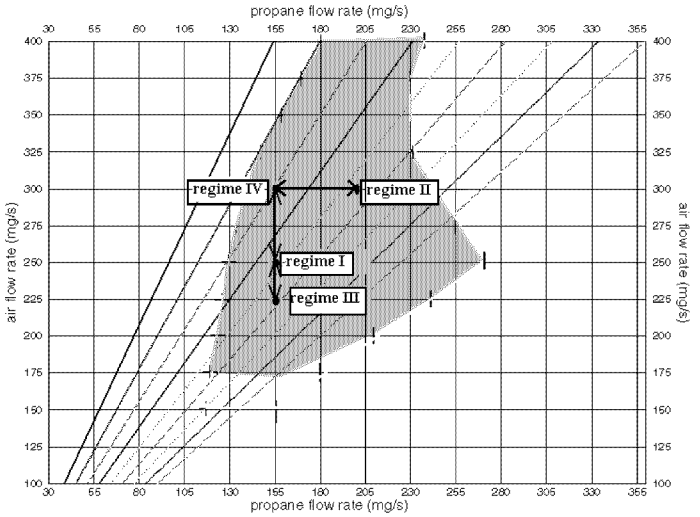

Fig. 4. Instability boundaries for a tube length of 750 mm. The unstable regime corresponds to the shaded zone. The command of instabilities in variable regimes (I, II, III, IV) is also shown [19].

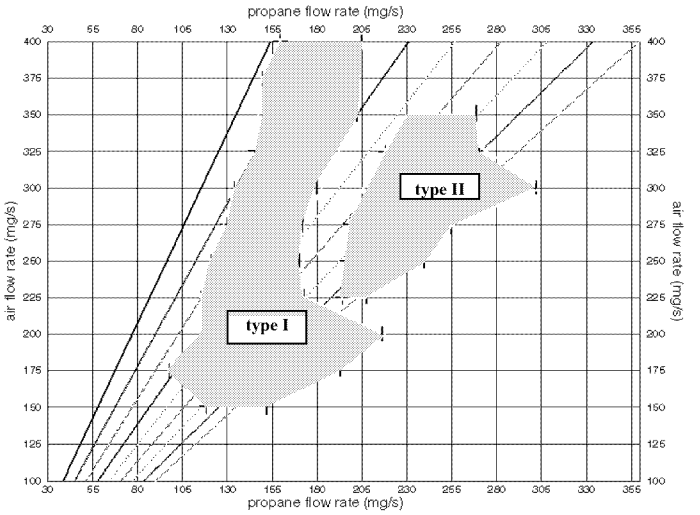

Fig. 5 - Instability boundaries for a tube length of 1m. Two unstable zones are shaded. The type I, which corresponds to weak values of propane mass flow rates, is similar to instabilities observed in Fig. 3 [19].

For a chamber length of 75 cm, power spectral densities of acoustic pressure or OH emission present a dominant peak of 145 dB/Hz at a frequency of 230 Hz. Other peaks of lower level are also observed.

For a tube length of 1m, two types of instabilities exist. The first one, which is observed for weak values of air mass flow rates, is similar to the instabilities encountered on a 75 cm chamber length. The dominant peak of 145 dB/Hz is also still present. This corresponds to the regime V. The second type of instability is encountered for air mass flow rates > 225 mg/sec and $\Phi > 1$ (regime VI). It is characterized by the presence of two peaks at 235 Hz and 460 Hz with 135 dB/hZ and 145 dB/Hz level respectively .

4 - Description of the Artificial Neural Networks (A.N.N.)

The ANN are sets of interconnected cells arranged in such a way that each cell receives its inputs from one or more cells and its output is sent, through weighted connections, to one or more cells. Hence, the ANN are multi-input-output (MIMO) signal processing, which operate nonlinear mapping between their inputs and outputs.The nature of the mapping depends on the ANN set of parameters, also called synaptic weights. These parameters are set up through a learning process. This consists in presenting to the ANN a sample set of input/output, called the training set, where the training algorithm iteratively adjusts the synaptic weights in order to obtain the desired output.

The multilayer feed-forward neural networks

Among different types of ANN, a multi-layer feed-forward networks (also called Multi-Layer Perceptron (MLP) is retained for this research. It is given in Fig. 6. It consists of an input layer, one or more hidden layer, and an output layer. In this study, we use one hidden layer feed-forward neural networks with one output.

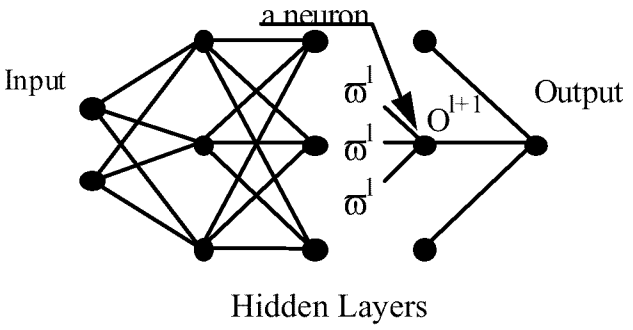

Fig. 6 -Scheme of a multi-layer Perceptron.

The cells in the hidden layer are called neurons. This element simply sums all the inputs multiplied by their respective synaptic weights. Then a nonlinear transfer function is applied to this sum. A bias term I_i^{hid} is also added to the input of each neuron. Let O_i^{hid} be the output of the i^{th} neuron of the hidden layer. We have :

$$O_i^{hid} = f\left(S_i^{hid}\right) = f\left(\sum_{j=1}^{Ninp} \varpi_{ij}^{hid} O_j^{inp} + I_i^{hid}\right)_{i=1,\ldots,N_{hid}}, \quad (1)$$

where f is the cell transfer function; S_i^{hid} is the input of the i^{th} neuron of the hidden layer; ϖ_t^{th} is the value of the weight of the connection between the j^{th} network input and the i^{th} neuron of the hidden layer; N_{hid} is the number of cells in the hidden layer. The choice of the transfer function is essential. It is often a non decreasing function of the total input of the cell. Here f is *tanh* (x) function. Its first derivative is strictly positive.

The output of the network is obtained by a linear combination of the outputs of the hidden neurons. Let O^{out} be the network's output, we have :

$$O^{out} = \sum_{i=1}^{Ninp} \varpi_i^{out} O_i^{hid} + I^{out}, \quad (2)$$

where ϖ_t^{th} is the value of the weight of the i^{th} hidden neuron and the output; I^{out} is also a bias.

The weight optimization problem

The training of an ANN consists in a search of the optimal weights that minimize the error between the desired and actual output of the training set.

The error function is defined as the sum of the square error :

$$J = \sum_{n=1}^{K} e^2(n) = \sum_{n=1}^{K} \left(d^n - O^{out,n}\right)^2, \quad (3)$$

where K is the number of examples of input/output in the training set. The desired and the network outputs at time n are d^n and $I^{out,n}$ respectively. The error J is a differentiable function of the weights. We use a back-propagation algorithm [24] which gives an estimate of the error function derivatives and that is less computationally expensive than feed-forward (Pineda [25]). Using the chain rule, the required partial derivatives in the backward direction (from outputs to inputs), are computed.

Let introduce the new variables :

$$\delta_i^{hid} = -\partial J / \partial S_i^{hid} ; \delta^{out} = -\partial J / \partial O^{out} . \qquad (4)$$

Using the chain rule :

$$\delta_i^{hid} = f'(S_i^{hid}) \sum_{k=1}^{K} \delta^{out} \varpi_i^{out} ; \delta^{out} = 2e(n) \qquad (5)$$

The partial derivative of the cost function takes the form :

$$\frac{\partial J}{\partial \varpi_{ij}^{hid,n}} = \left(\frac{\partial J}{\partial S_i^{hid}} \right) \left(\frac{\partial S_i^{hid}}{\partial \varpi_{ij}^{hid,n}} \right) = -\delta_i^{hid} O_j^{inp} . \qquad (6)$$

The weights and the bias are updated using the momentum technique [24]. This method tries to avoid oscillations found in gradient descent algorithm. The weights are computed with the relation :

$$\varpi_{ij}^{l,n+1} = \varpi_{ij}^{l,n} + \eta \delta_i^{l+1,n} O_j^{l,n} + \alpha \left(\varpi_{ij}^{l,n} - \varpi_{ij}^{l,n-1} \right) \qquad (7)$$

with $\alpha \in [0,1]$. This algorithm accelerates the convergence of gradient method during "steady downhill" descent. Moreover, it presents a stabilizing effect in regions where the gradient oscillates. However, the choice of α and η is difficult. They are adjusted by a process of trial and error.

The neural control scheme

We present here the Internal Model Control System (ICMS). We are interested to a single input output process. The methods relies on the assumption that the process can be described as follows :

$$y_p(n) = h\left[y_{p,n-1}, \ldots, y_{p,n-N_y}, u_{n-1}, \ldots, u_{n-N_u} \right] + w(n), \qquad (8)$$

where y_p is the output of the process; u, the control input; h, an unknown nonlinear function which represents the plant dynamic; w, the noise measurement. The controller objective is to provide the correct control input to drive a nonlinear plant from an unstable to a stable regime. Adjustment of parameters is described in details in [19,20]. Tests have first been made on a numerical signal generated by solving a simplified nonlinear model of combustion instabilities [1,25,26].

The I.C.M.S. is described in Fig. 7. On one hand, the Internal Model (IM) is trained before the control sequence to approximate the unknown function h. On the other hand, the controller continuously adjusts the weights in order to minimize the distance between the IM and the desired output. This forces the controller to represent the inverse of the IM. Therefore, if the IM is good, the process will tend to make the plant output to follow the desired regime.

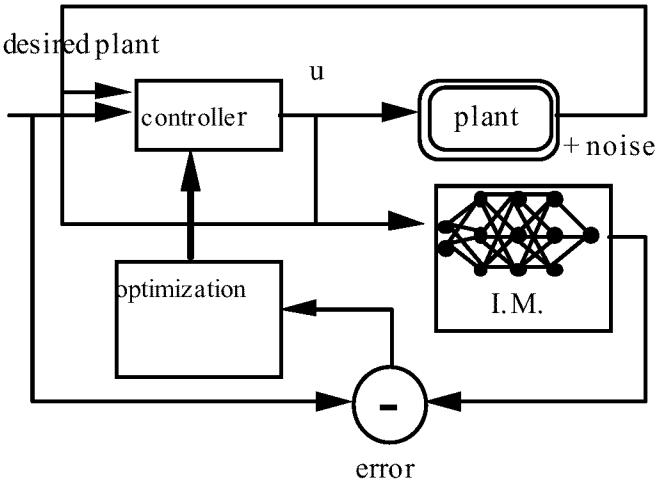

Fig. 7 - Internal Model Control System (I.M.C.S.).

The objective of this study is to minimize the rms value of pressure oscillation. The desired output is obviously $y_d = 0$. Let e_n be the difference between the desired and IM outputs at time n. We have :

$$\varepsilon_{n+1}^2 = \left(y_{IM}(n+1) - y_d(n+1)\right)^2 = y_{IM}^2(n+1). \qquad (9)$$

Let Ω_C, the set of weights of the controller, which defines the value of the control input. During control, the weights are adjusted in order to minimize the instantaneous square error given by eq. (10). The weight correction $\Delta\Omega_C$ is computed using the gradient descent technique. For real time control purposes, the correction is computed through the following relation:

$$\Delta\Omega_c = -\mu_c \left(\frac{\partial \varepsilon_{n+1}^2}{\partial y_{md}(n+2)}\right)\left(\frac{\partial y_{md}(n+2)}{\partial u(n+1)}\right)\left(\frac{\partial u(n+1)}{\partial \Omega_n}\right) , \qquad (10)$$

where $\varepsilon_{n+1}^2 = y_{md}^2(n+2)$.

Identification of the internal model

The burner is excited by sending acoustic sine waves to the loudspeakers at frequencies close to those of the instabilities. This response of the system is delivered by a microphone mounted downstream from the porous plate. The excitation signal and the response of the burner provide the training set for the identification process. The selection technique of the model is described in details in [19]. The number of parameters to adjust is less than 20.

5 - Results with control [19]

In all these experiments, the constant in eq. (10) is $\mu_C = 0.05$. In this test, the OH signal is used to detect instabilities.

Figures 8, 9 and 10 give examples of spectra obtained with control. Compared to the situation without control, considerable attenuation is observed for regime I (Fig. 8); V (Fig. 9); VI (fig. 10). Similar results are obtained with microphone and photomultiplier.

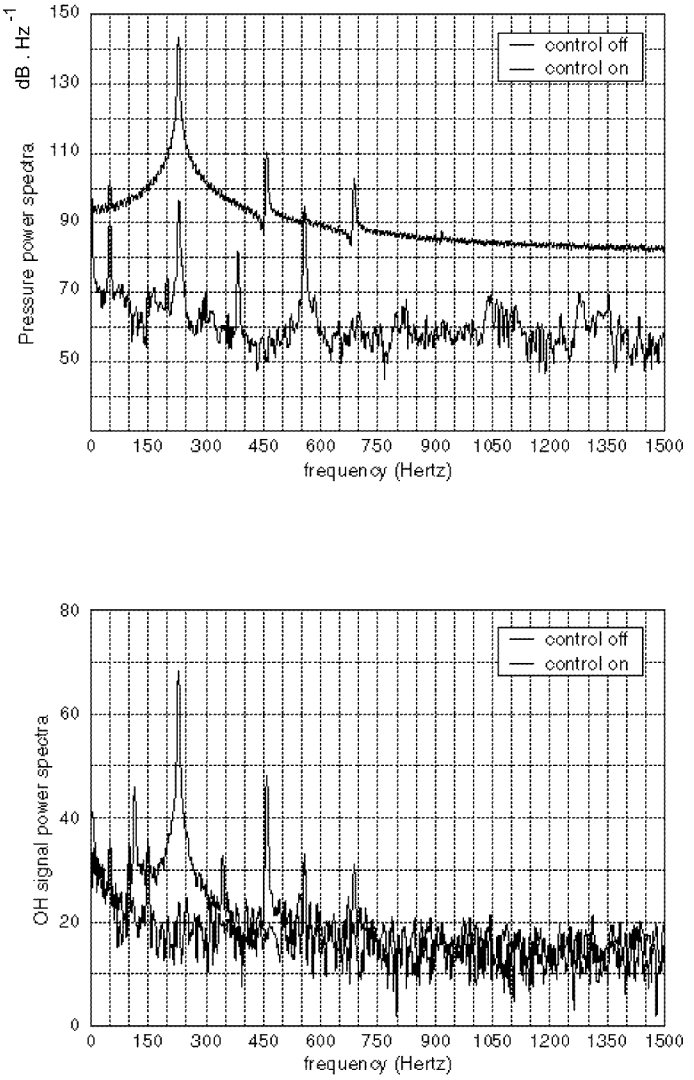

Fig. 8 - Power spectral densities of pressure and OH emission signals for regime I, with and without control [19].

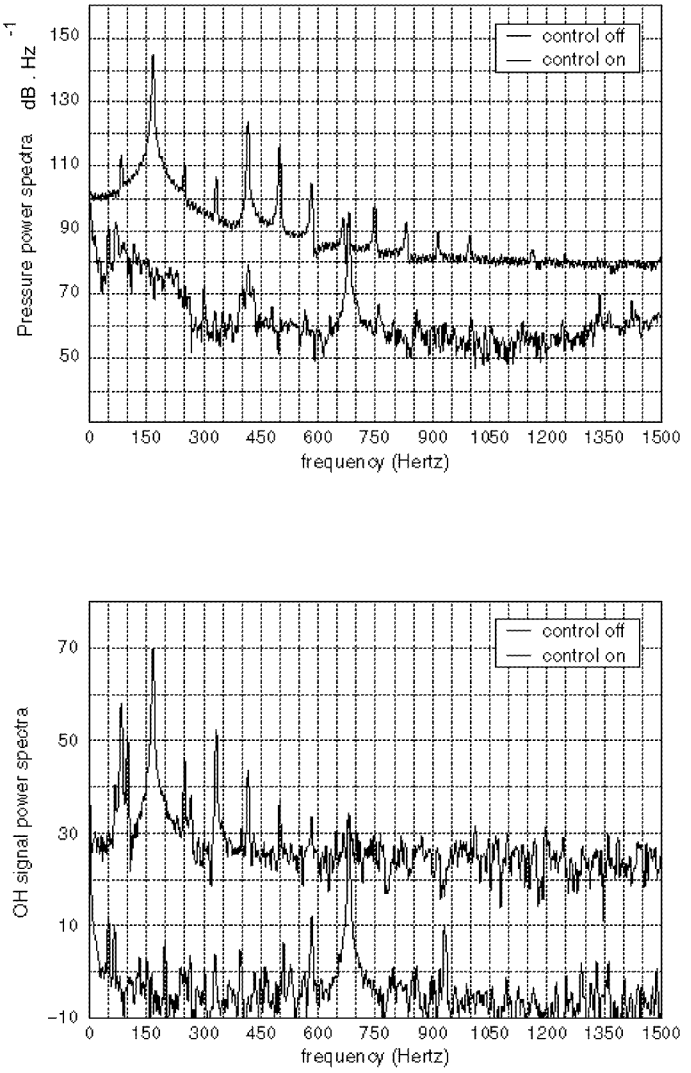

Fig.9 - Power spectral densities of pressure and OH emission signals for regime V, with and without control [19].

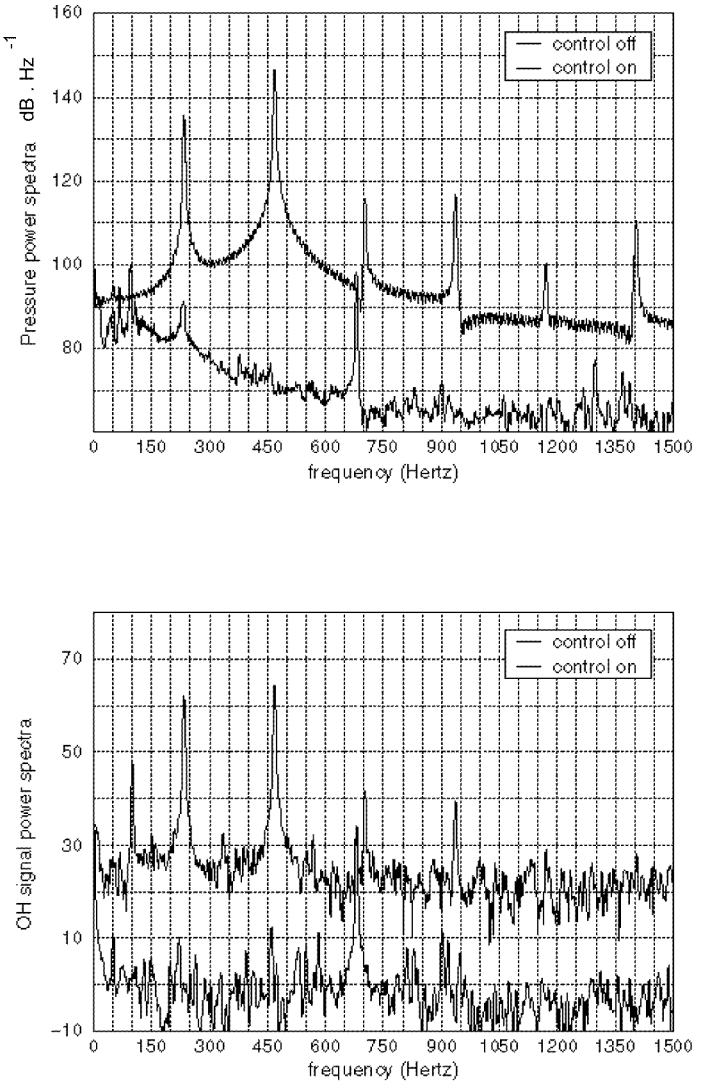

Fig. 10 - Power spectral densities of pressure and OH emission signals for regime VI, with and without control [19].

Figure 11 shows the temporal signals during a control sequence. The controller is turned on at $t \approx 1.65$ s. A subsequent damping of the instabilities is obtained in a short time ($t \approx 1.9$ s). Before control, the actuator signal amplitude is weak. After the control is on, the actuation signal increases fastly then it decreases to a low level. When the controller is off, the instabilities starts again, proving its efficiency (Fig. 12).

The possibilities of this control system have also been tested when changing operating conditions during a control sequence. The changes performed follow the path shown in Fig. 4. The IM identification has been performed only for conditions corresponding to regime I. Fig. 13 shows successive power spectral densities of the pressure signal with and without control. Global attenuation is observed. Moreover, reductions of instabilities up to 60 dB/Hz have been obtained. This again proves the efficiency of the active control of the IMCS.

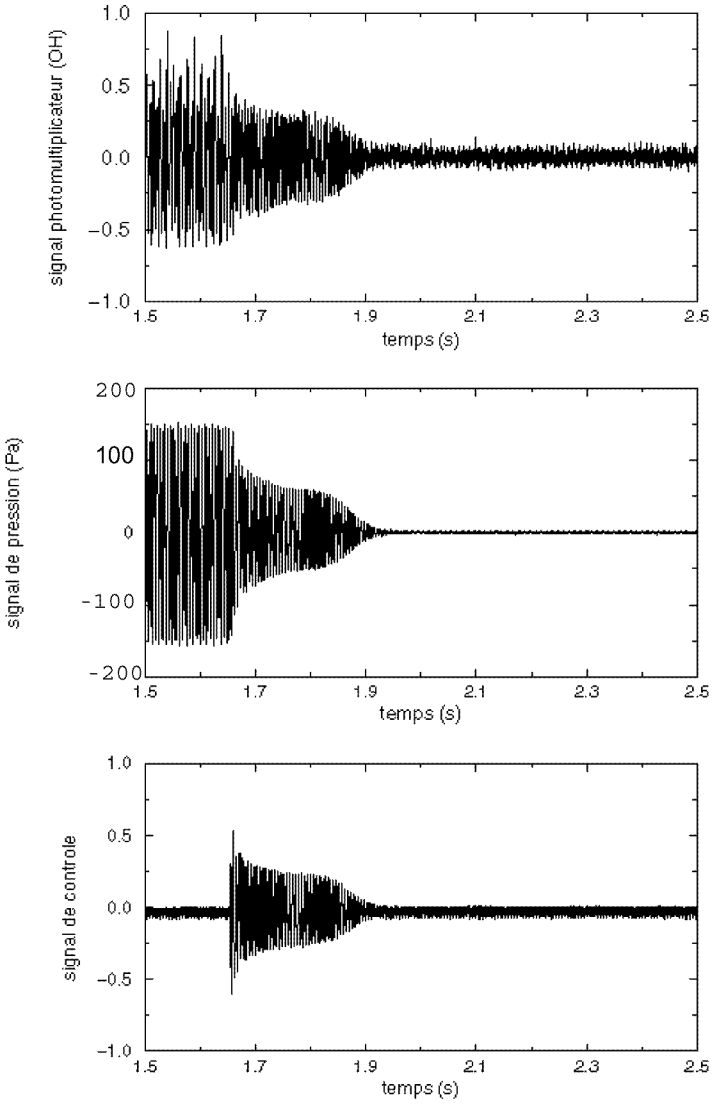

Fig. 11 - Temporal signal of pressure, OH emission and control obtained during a sequence of control of instabilities for regime VI. During this experiment, photomultiplier signal is used at the loop entry [19].

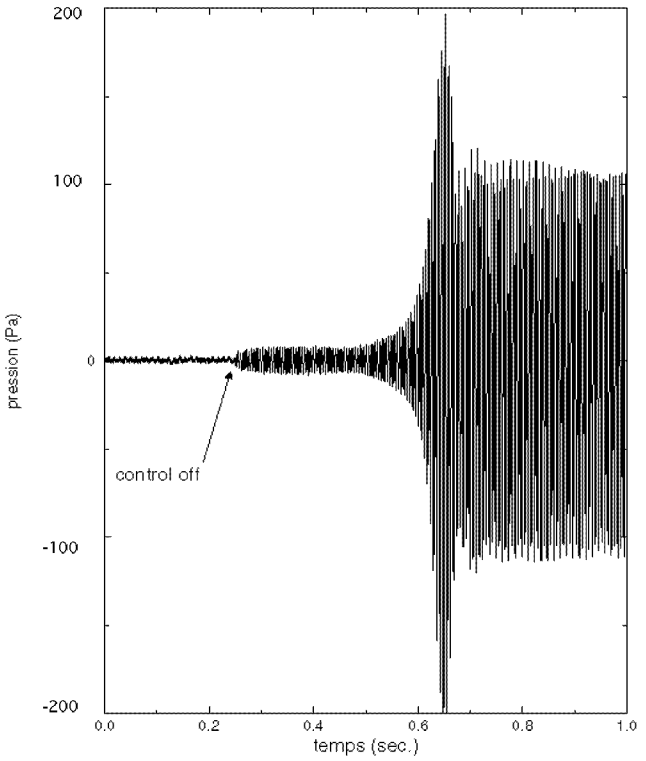

Fig. 12 - Temporal signal of pressure obtained when the control sequence is stopped. The instabillity starts again, proving the control algorithm efficiency [19].

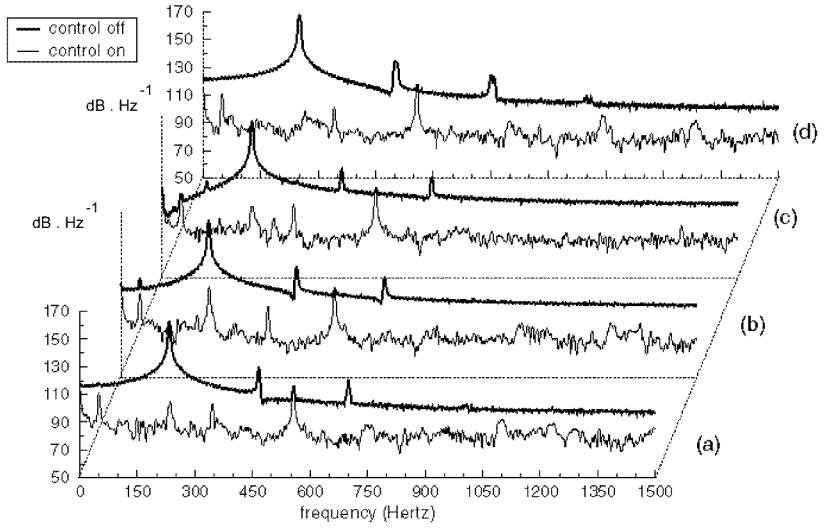

Figure 13 - Microphone signal power spectral density without and with control. Different changing operating conditions, indicated in Fig. 4, which corresponds to regimes I to IV, are considered. a) regime III; b) regime I; c) regime IV; d) regime II [19].

Conclusion

In this paper, we have described a Rijke tube and an active control of combustion instability based on neural networks technique. This burner, tested for two lengths and different operating conditions, shows combustion instabilities of level up to 145 dB/Hz. The pressure signals produced by a microphone or the OH emission signals of a photomultiplier are correctly predicted by the Internal Model of the neural network. A control algorithm is also proposed. It is an efficient device which is able to control the burner for fixed or varying operating conditions. Pressure level attenuation up to 60 dB/Hz have been obtained. This result proves the ability of Artificial Neural Networks to approximate noisy instability signals and to control it. The following investigation would consist, on one hand, in testing this ANN techniques on aeronautical powerplant; on the other hand, in defining a new actuator for this type of motor.

Acknowledgments :

This work has received financial support from ONERA. Real time learning and control algorithms, in assembly langage on PC computer, have been written by Kurtosis society.

References

[1] Culick, F.E.C. AGARD conference Proceedings, n°450, 1988.

[2] Williams, F.A., *Combustion Theory*, 2nd ed., Benjamin Cummings, Menlo Park, CA, 1985.

[3] Poinsot, T. "Analyse des Instabilités de Combustion de Foyers Turbulents Prémélangés", Thèse d'Etat , University of Paris - Sud, Orsay, France, Feb. 2 nd 1987.

[4] Laverdant, A.M. "Contribution À l'Étude des Instabilités de Combustion des Foyers Aérobies", Thèse d'Etat , University of Rouen, France, 1991.

[5] Dines, P.J., "Active Control of Flame Noise", Ph. D. Thesis, Cambridge University, 1983.

[6] Heckl, M.A. "Heat Sources in Acoustic Resonator", Ph. D. Thesis, Cambridge University, 1985.

[7] Lang, W., Poinsot, T. and Candel, S.M., Comb. & Flame, 70, 281-289, 1987.

[8] Crocco, L. Tenth Symposium (International) on Combustion, The Combustion Institute, Pittsburgh, PA, 1965, 1101-1128.

[9] MC Manus, K.R., Poinsot, T. and Candel, S.M., Prog. Energy & Combust. Sci., 19, 1-29, 1993.

[10] Huynh-Huu, C., Le Helley, P., Poinsot, T. Esposito, E. and Candel, S.M., "Contrôle Actif Adaptatif des Instabilités de Combustion", Final Rept. DRET 89-262, june 30 th 1993 and E.M2.C. lab. Rept. C.N.R.S., Ecole Centrale de Paris.

[11] Billoud, G., Galland, M.A., Huynh-Huu, C. and Candel, S.M., Combust. Sci. & Tech., 81, 257-283, 1992.

[12] Widrow, B., *Adaptive Filters*, Aspects of Network & System Theory, Holt Rinehart, New-York, 1971.

[13] Neumeier, Y. and Zinn, B.T., AIAA Paper n°96-0758, 34 th Aerospace Sci. Meeting, Jan. 1996.

[14] Yu, K.H., Wilson, K.J. et Schadow, K.C., "On liquid-fueled active combustion control: instability suppression in dump combustors", ISABE paper n° 99-71184 et AIAA paper n° 99-34185, 1999.

[15] Bishop, C.M., *Neural Networks for Pattern Recognition*, Clarendon Press, Oxford, 1995.

[16] Hunt, K.J., Sbarbaro, D., Zbikowski, R., and Gawthrop, P.J., Automatica, 28, 359-366, 1989.

[17] Rijke, P.L. Phil. Mag. ,17, p. 419, 1859.

[18] Raun, R.L., Beckstead, M.W., Finlinson, J.C. and Brooks, K.P. Prog. in Energy & Comb. Sci., 19, 313-364, 1993.

[19] Blonbou, R. “Commande des Instabilités de Combustion par Réseaux de Neurones”, Ph. D Thesis, Paris Sud University, France, 1999.

[20] Blonbou, R., Laverdant, A., Zaleski, S. and Kuentzmann, P. to be published in Comb. Sci & Tech.

[22] Diederichsen, J. and Gould, R.D., Comb. & Flame, 9, 25-31, 1965.

[23] lord Rayleigh, J.W.S., Roy. Inst. Proc., VIII, 536-542,1878.

[24] Rumelhart, D.E., Hinton, G.E. and Williams, R.J., *Learning Internal Representations by Error Propagation*, in Parallel Distributed Processing : Exploration in the Microstructure of Cognition, Rumelhart, J.L. Mc Clelland and the PDP research group (eds.), Vol. I : Foundations, MIT Press, Cambridge, Mass, 1986.

[25] Pineda, F.J. Neural Comp., 1, 161-172, 1989.

PAPER -21, A. Laverdant

Question (B. Zinn, USA)

Has the neural net ever amplified the instability during the transient process during which the neural net is determining the optimal control parameters?

Reply

Generally, the neural net has given a precise prediction of the instability signal during the transient process. When the identification process is correctly done, the controller damps the instabilities. However, on real-time applications, algorithmic instabilities can occur during the transient process.

Question (A. Annaswamy, USA)

Can you provide a comparison between neural net control and other linear control?

Reply

Classical active control damps one peak and amplifies another one. The neural network predicts instability from noisy signals with a low global error. Therefore, the adaptive control is efficient in real-time for stabilizing all modes.

Question (F. E. C. Culick, USA)

Why are the fundamental frequencies for the two tubes approximately the same even though the lengths are in the ratio 1:0.75? Also, it seems that the your data show consistently that the noise level is higher when the tube is controlled. Is this a correct inference? (If so, why?)

Reply

The fundamental frequencies are different: 160 Hz for a 75 cm tube and 230 Hz for a 1m tube. The noise level is reduced at least 20 dB when the control is on.

Question (M. Mettenleiter, France)

Did you try to analyze the mapping function of your neural network?

Reply

No classical analysis of the mapping of the neural net has been done yet (eg, gain and phase plots). However, the neural net model has a nonlinear transfer function and its accuracy has been evaluated in the time domain by comparing the combustor response to open loop excitation with the neural net response to the same excitation.